

Measurement of the internal magnetic field of plasmas using an alpha particle source

S. J. Zweben,^{a)} D. S. Darrow, and P. W. Ross
Princeton Plasma Physics Laboratory, Princeton, New Jersey 08540

J. L. Lowrance and G. Renda
Princeton Scientific Instruments, Inc., Monmouth Junction, New Jersey 08852

(Presented on 19 April 2004; published 5 October 2004)

The internal magnetic fields of plasmas can be measured under certain conditions from the integrated $v \times B$ deflection of MeV alpha particles emitted by a small radioactive source. The alpha source and large-area alpha particle detector would be located inside the vacuum vessel but outside the plasma. Alphas with a typical energy of 5.5 MeV (^{241}Am) can reach the center of almost all laboratory plasmas and magnetic fusion devices, so this method can potentially determine the $q(r)$ profile of tokamaks or spherical toris (STs). Orbit calculations, background evaluations, and conceptual designs for such $\alpha v \times B$ (or “AVB”) detector are described. © 2004 American Institute of Physics. [DOI: 10.1063/1.1779610]

I. INTRODUCTION

The internal magnetic fields of fusion plasmas have been measured through the motional Stark effect,¹ the Zeeman effect,² and Faraday rotation.^{3,4} These diagnostics have succeeded in measuring the poloidal magnetic field profile of tokamaks but are difficult to implement, especially on smaller devices, due to their complexity and cost.

Previously, a collimated beam of injected fast ions was used to measure the $q(r)$ profile in the ATC tokamak,⁵ and collimated detectors were proposed to measure the $q(r)$ profile using 3 MeV proton emission.⁶ Heavy ion beam probes (HIBPs) have also been considered for internal plasma magnetic field measurements; for example, the light emission from a HIBP can be used to map out the beam trajectory inside the plasma, and thus measure the $v \times B$ deflection and local B field seen by the beam.⁷ Another recent proposal is to use a high-powered short-pulse laser to generate ≈ 100 keV electrons inside the plasma,⁸ which would then follow the magnetic field line to the wall, such that the wall x-ray burst could help reconstruct internal magnetic field to some extent.

This article describes the potential use of an alpha particle source to measure the internal magnetic structure of fusion plasmas. This source would most likely be ^{241}Am with a strength ≈ 1 mCi and an alpha energy of ≈ 5.5 MeV. The gyroorbits of these alphas can reach the center of a magnetized plasma of magnetic field “ B ” and radius “ a ” roughly whenever $B(\text{kG}) \cdot a(\text{m}) \leq 3$. This is condition is marginally satisfied for National Spherical Torus Experiment (NSTX) at the Princeton Plasma Physics Laboratory (PPPL) where $B \approx 4.5$ kG, $a \approx 0.65$ m, as shown below. It is easily satisfied for most smaller magnetic fusion devices and laboratory plasmas; however, it is not satisfied on large fusion devices such as the Joint European Torus (JET), which are designed to confine 3.5 MeV alpha particles.

II. ALPHA PARTICLE ORBIT CALCULATIONS

The $\alpha v \times B$ (AVB) alpha particle source would be located inside the vacuum vessel but well outside the plasma. The alphas would first pass through a highly collimated aperture to fix their initial direction, and then travel to the plasma center and back out again while integrating the local $v \times B$ force. Their impact location would be measured by a large area detector at the wall.

Alpha particle orbits for an AVB measurement in NSTX are illustrated in Fig. 1. Here an alpha source of energy 5.5 MeV is located $\approx 45^\circ$ below the outer midplane, and three alpha particle trajectories are plotted for each of two different $q(r)$ profiles. The three orbits have poloidal launch angles of $\theta = 0^\circ$, 10° , and 20° and a toroidal launch angle of $\varphi = 28^\circ$ (i.e., nearly radial). This discharge (No. 104033) had $B = 4.5$ kG and $I = 770 \pm 10$ kA, and the two $q(r)$ profiles had $q(0) \approx 1.0$ (solid lines) or $q(0) \approx 1.7$ (dashed lines) within $r/a \approx 0.5$, both with the same $q(a) \approx 8$. This difference in $q(a)$ profiles did not significantly affect the orbits in the poloidal plane (left), but there was a clear difference in the toroidal impact location between the two $q(r)$ profiles (right).

Figure 1 illustrates the main principle of this diagnostic. Alpha particles which are launched nearly perpendicular to the toroidal field will have gyroorbits which tend to remain perpendicular to the plane of the total B field; thus, the plane of their orbit will rotate along with the (local) magnetic field line angle. Thus the (average) poloidal magnetic field line angle can be measured by the toroidal impact position of the alpha orbits. The poloidal impact position of the orbit is largely determined by the toroidal field, and so does not vary much with the $q(r)$ profile.

One limit to the accuracy with which the $q(r)$ profile can be determined is the initial spread in toroidal launch angles at the alpha source. Figure 2 shows a plot of the alpha particle impact location for the orbits of Fig. 1, along with the impact locations at the edges of an assumed (square) source

^{a)}Electronic mail: szweben@pppl.gov

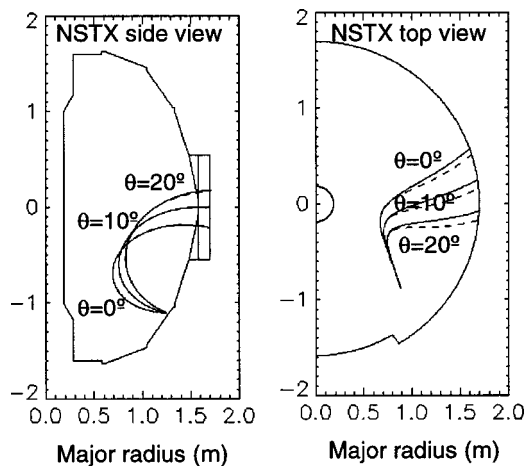


FIG. 1. Alpha particle orbit calculations for a realistic magnetic geometry in NSTX. The alphas of 5.5 MeV are launched $\approx 45^\circ$ below the outer midplane at three different poloidal angles $\theta=0^\circ$, 10° , and 20° , all with a toroidal launch angle of $\chi=28^\circ$ (i.e., nearly radial). The solid lines are for a $q(r)$ profile with $q(0)=1.7$ and the dashed line for $q(0)=1.0$, both with $q(a)=8$.

aperture for each. The aperture angles for Fig. 2 were chosen so that the range of toroidal impact location due to the finite aperture size would be significantly less than the difference in toroidal impact locations between the two $q(r)$ profiles. For this case these angles were $\Delta\theta=5^\circ$ (in the poloidal direction) and $\Delta\varphi=0.6^\circ$ (in the toroidal direction). A measurement with these apertures could distinguish these $q(r)$ profiles.

Simple analytic estimates⁹ show that accuracy with which the (orbit-averaged) angle of B can be measured, given a toroidal aperture angle $\Delta\varphi$, is roughly $\Delta\chi \approx (\pi/2)\Delta\varphi$, which is in rough agreement with Fig. 2 and with a cylindrical model calculations of $q(r)$ profile variations in NSTX. Since the alpha impact locations for various $q(r)$ profiles form smooth curves when the poloidal launch angle is varied, a source aperture with a continuous slit in the poloidal direction would allow increased signal without significantly degrading the observable variation due to $q(r)$.

The requirement for spatial resolution of B inside the

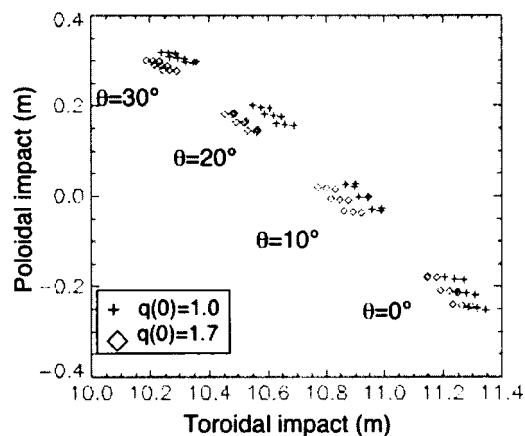


FIG. 2. Variation of the alpha particle wall impact location for the cases of Fig. 1. For each $q(r)$ and launch angle θ there nine points corresponding to the center and corners of the assumed alpha source aperture. For this plot, these aperture angles were $\Delta\theta=5^\circ$ (in the poloidal direction) $\Delta\varphi=0.6^\circ$ (in the toroidal direction).

TABLE I. Alpha source and detector requirements.

Alpha source energy: $\approx 5.5 \pm 0.1$ MeV
Alpha source strength: ≈ 1 mCi (3.7×10^7 /s)
Alpha detector pixel size: ≈ 1 cm
Alpha detector size: ≈ 40 cm \times 40 cm
Alpha detector energy resolution: $\approx 50\%$
Alpha particle count rate $\approx 10^4$ /s/aperture

plasma implies a need for multiple alpha source apertures each defining a distinct alpha orbit trajectory, e.g., with varying initial alpha angles θ and φ , and/or alpha energy E . A single large area AVB detector could probably identify the impact locations for ≈ 10 source apertures. Thus it seems possible to unfold up to ≈ 10 spatially resolved points on the $q(r)$ profile with a single AVB detector.

III. ALPHA DETECTOR DESIGN

The AVB alpha detector would be a two dimensional (2D) position sensitive detector with sufficient spatial resolution to localize the alpha impact locations from an alpha source with ≈ 10 apertures. For a conceptual design we assume an ^{241}Am source of $\approx 5.5 \pm 0.1$ MeV alphas with a strength of ≈ 1 mCi, or 3.7×10^7 alphas/s (e.g., from Isotope Products, Inc). The alpha flux through a single aperture slit with $\Delta\theta=10^\circ$ (in the poloidal direction) and $\Delta\varphi=0.6^\circ$ (in the toroidal direction) would be $\approx 10^4$ alphas/s. To localize the alpha impacts from a single aperture would require ≈ 100 counts, thus a typical measurement timescale would be ≈ 10 ms.

The required detector spatial resolution (i.e., pixel size) is determined by the desired $q(r)$ profile resolution. For the NSTX case of Fig. 2, the two $q(r)$ profiles are separated by ≈ 5 cm at the detector, so a spatial resolution of ≈ 1 cm would be sufficient. The size of the AVB detector is determined by the range of $q(r)$ and B field variations to be measured in a given device. For the NSTX cases of Fig. 2 the detector should have a size of ≈ 40 cm \times 40 cm.

These AVB source and detector requirements for NSTX are summarized in Table I. Assuming a design with 10 slit apertures as described above, the total alpha count rate would be $\approx 10^5$ alphas/s. For other devices the required detector resolution and size will scale roughly linearly with the alpha gyroradius. As discussed below, background discrimination may require a modest amount of alpha energy resolution from this detector.

The main background in deuterium fusion plasmas such as NSTX would be the escaping flux of D-D fusion products from the plasma, including the 1 MeV triton, the 3 MeV proton, and the 0.8 MeV ^3He from D-D reactions (the D-T and D- ^3He burnup products should be negligible for plasmas of interest). The 1 MeV triton and 0.8 MeV ^3He can be blocked by a $5 \mu\text{m}$ gold foil covering the detector, after which the 5.5 MeV alpha will still have ≈ 3 MeV.¹⁰ However, the range of the 3 MeV proton in gold is $\approx 30 \mu\text{m}$ so this gold layer will not stop the proton. Since the gyroradius of the 3 MeV proton is nearly the same as a 5 MeV alpha particle, a large fraction of D-D protons reach the wall

TABLE II. AVB detector backgrounds for three devices.

Parameter	ET (UCLA)	MST (Wisc.)	NSTX (PPPL)
T_e (keV)	≈ 0.5	≈ 0.5	$\approx 0.5(\text{OH})-2(\text{NBI})$
$n_c(10^{13} \text{ cm}^{-3})$	≈ 0.2	≈ 1	$\approx 1(\text{OH})-3(\text{NBI})$
neutrons/s	$\approx 10^6$	$\approx 10^8$	$\approx 10^9(\text{OH})-10^{14}(\text{NBI})$
(protons/ α) ^a	< 0.01	$\sim 0.1-1$	$\sim 1(\text{OH})-10^5(\text{NBI})$
(x-ray/ α) ^b	~ 0.1	~ 1	$\sim 1(\text{OH})-10^5(\text{NBI})$

^aNumber of 3 MeV protons/number of AVB alphas onto detector.

^bX-ray energy flux/AVB alpha energy flux behind 5 μm gold foil.

whenever the AVB alpha particle can reach the plasma center. Therefore the escaping 3 MeV proton flux can be a significant background whenever the D–D fusion rates becomes very much larger than the AVB alpha source rate.

Estimates of the ratio of the 3 MeV proton rate to the AVB alpha rate for three plasma devices is given in Table II, assuming an AVB detector design similar to that of Table I. The proton background should be negligible for low temperature (or hydrogen fueled) devices like the electric Tokamak (ET). However, for higher temperature devices like madison symmetric torus (MST) or NSTX this background will make the AVB measurement more challenging. One detection strategy is to discriminate the AVB alphas from the protons through pulse height analysis; for example, in a silicon detector just thick enough to stop a 3 MeV AVB alpha ($\approx 12 \mu\text{m}$) the 3 MeV proton will deposit ≤ 0.3 MeV. Thus the pulse height discrimination of the alphas from the protons should be relatively easy, at least when the proton count rate is ≤ 10 times the alpha count rate.

The only other significant background should be due to x rays emitted from the plasma. However, a gold coating or foil over the detector would block most of the plasma x rays (along with visible and ultraviolet light); for example, the fraction of thermal plasma x-ray energy passing through a 5 μm gold foil would be $\approx 10^{-6}$ for $T_e=0.5$ keV, 10^{-4} for $T_e=1$ keV, and $\approx 10^{-2}$ for $T_e=2$ keV.¹⁰ Thus the x-ray background for the devices of Table II would be negligible for ET, moderate for MST, and ohmic NSTX plasmas, but large for neutral beam injection (NBI) heated NSTX plasmas. However, this x-ray background will consist of a very large number of very small pulses (≤ 1 keV), so a good pulse height discrimination system might be able to eliminate most of this x-ray background.

Turning to detector implementation, the alpha detection requirements of Table I can certainly be met by an array of cm-discrete silicon diode detectors (e.g., ORTEC Ultra series). However, a 40×40 array such detectors would be prohibitively expensive and complicated to monitor.

A simpler technique would be to use an optically coupled scintillator screen. It is well known that thin powdered phosphors such as ZnS can detect single alpha particles, and screens of 40×40 cm can be easily made. The crystal size of these phosphors is typically only a few μm , so the alpha energy resolution will be poor; however, if the backgrounds are relatively small this should be acceptable.

The detector spatial resolution can be ≈ 0.1 cm, and the response time (depending on phosphor type) can be $\approx 1-30 \mu\text{s}$. The screen can be viewed from behind by a single large lens, or if space is limited, by an array of fiber optically coupled “funnel/cones” similar to that employed in Cerenkov radiation detectors. Most likely thousands of single alpha impacts can be seen simultaneously on such a screen using an intensified video camera with a nominal integration time of 16 ms/frame.

Another possible detection technique would be a large-area position sensitive amorphous silicon detector. For example, $40 \text{ cm} \times 40 \text{ cm}$ amorphous silicon diode arrays with 200 μm spatial resolution are already used for industrial and medical x-ray imaging applications (e.g., from Perkin Elmer). There is also ongoing work to develop large area amorphous silicon detector arrays for particle detection in physics experiments.¹¹ An amorphous silicon detector array should have much better energy resolution than a phosphor screen; however, signal handling at a total count rate of ≈ 100 kHz may be difficult.

IV. OTHER APPLICATIONS

Although the backgrounds are high when $T_e(0) > 1$ keV, this diagnostic might be able to make an edge qr measurement by using movable baffles to block the x rays and 3 MeV protons from the plasma center.⁹ In this case the detector would see only alphas passing through the edge and incident onto the detector at a small angle, along with the local backgrounds from this edge region. The AVB diagnostic could also be used to measure the magnitude of the internal B in “self-organized” plasmas like field-reversed configurations (FRCs) or high β STs,¹⁰ or to map the 3D magnetic field structure in stellarators. Finally, if alpha sources can be found with a strength of ≈ 1 Ci (instead of 1 mCi), it might be possible to measure internal magnetic field fluctuations this way.

ACKNOWLEDGMENTS

The authors thank D. Johnson and P. Efthimion of PPPL for supporting this study, S. Kaye for information about NSTX neutron rates, and P. Schoch for discussions about the heavy ion beam probe. This work was performed under DOE Contract No. DE-AC02-76CHO3073.

¹S. Reyes Cortes *et al.*, Rev. Sci. Instrum. **74**, 1596 (2003).

²D. M. Thomas, Rev. Sci. Instrum. **74**, 1541 (2003).

³D. L. Brower *et al.*, Rev. Sci. Instrum. **74**, 1534 (2003).

⁴K. C. Lee *et al.*, Rev. Sci. Instrum. **74**, 1621 (2003).

⁵R. J. Goldston, Phys. Fluids **21**, 2346 (1978).

⁶W. W. Heidbrink *et al.*, Rev. Sci. Instrum. **56**, 501 (1985).

⁷D. R. Demers *et al.*, Rev. Sci. Instrum. **74**, 2103 (2003).

⁸H. S. McLean *et al.*, Rev. Sci. Instrum. **74**, 1547 (2003).

⁹S. J. Zweben *et al.*, Princeton Plasma Physics Laboratory Report No. 3958 (2004).

¹⁰NIST (<http://physics.nist.gov/PhysRefData>)

¹¹C. Hordequin *et al.*, Nucl. Instrum. Methods Phys. Res. A **456**, 284 (2001).